BJP British Journal of Pharmacology

DOI:10.1111/bph.12547
www.brjpharmacol.org

RESEARCH PAPER

A novel phenylcyclohex-1-enecarbothioamide derivative inhibits CXCL8-mediated chemotaxis through selective regulation of CXCR2-mediated signalling

Helen Ha[1], Tim Bensman[2]*, Henry Ho[2]*, Paul M Beringer[2] and Nouri Neamati[1]

[1]*Department of Pharmacology and Pharmaceutical Sciences, School of Pharmacy, University of Southern California, Los Angeles, CA, USA, and* [2]*Department of Clinical Pharmacy and Pharmaceutical Economics & Policy, School of Pharmacy, University of Southern California, Los Angeles, CA, USA*

Correspondence
Nouri Neamati, Department of Medicinal Chemistry, College of Pharmacy University of Michigan, North Campus Research Complex 2800 Plymouth Road, Bldg 520, Room 1363, Ann Arbor, MI 48109-2800, USA. E-mail: neamati@umich.edu

*These authors contributed equally to this work.

Keywords
CXCR2; CXCL8:IL-8; β-arrestin; inflammation; chemotaxis; receptor internalization

Received
1 March 2013
Revised
26 November 2013
Accepted
2 December 2013

BACKGROUND AND PURPOSE

Since the CXC chemokine receptor CXCR2 and its cognate ligand CXCL8 (IL-8) critically regulate neutrophil trafficking during inflammation, they have been implicated in a number of inflammatory lung diseases. Several CXCR2 antagonists have been described and the blockade of CXCR2 has shown promise in pre-clinical disease models and early clinical trials. However, given its potential, there are fewer distinct classes of antagonists of CXCR2 than of other clinically relevant molecular targets. Thus, we sought to identify additional classes of compounds that alter CXCR2 function.

EXPERIMENTAL APPROACH

We used the CXCR2 Tango™ assay to screen an in-house library of highly diverse chemical compounds. CX4338 [2-(benzylamino)-4,4-dimethyl-6-oxo-*N*-phenylcyclohex-1-enecarbothioamide] was identified from our screen and additional studies to characterize the compound were performed. Receptor internalization and second-messenger assays were used to assess the effects of CX4338 on CXCR2-mediated signalling. Wound healing, transwell cell migration and LPS-induced lung inflammation in mice were used to determine the *in vitro* and *in vivo* effects of CX4338.

KEY RESULTS

CX4338 selectively inhibited CXCR2-mediated recruitment of β-arrestin-2 and receptor internalization, while enhancing CXCR2-mediated MAPK activation. Additionally, CX4338 inhibited CXCL8-induced chemotaxis in CXCR2-overexpressing cells and human neutrophils. *In vivo*, CX4338 significantly reduced neutrophils in bronchoalveolar lavage induced by LPS in mice.

CONCLUSIONS AND IMPLICATIONS

A novel compound CX4338 inhibited CXCR2-mediated cell migration with a mechanism of action not previously reported. Also, selective inhibition of CXCR2-mediated β-arrestin-2 activation is sufficient to inhibit CXCL8-mediated chemotaxis.

Abbreviations

BAL, bronchoalveolar lavage; CF, cystic fibrosis; COPD, chronic obstructive pulmonary disease; CX4338, 2-(benzylamino)-4,4-dimethyl-6-oxo-N-phenycyclohex-1-enecarbothioamide; GRK6, G-protein receptor kinase 6; NOX, NAPDH-oxidase

Introduction

The CXC chemokine receptor CXCR2 is expressed on immune cells, such as neutrophils, monocytes, basophils and lymphocytes, as well as pulmonary endothelium and bronchial epithelia, and plays a critical role during acute and chronic inflammation by mediating neutrophil activation and migration to sites of infection (Baggiolini *et al.*, 1997). CXCR2 is activated by all chemokines containing the glutamate, leucine and arginine (ELR) motif, such as CXCL8 (IL-8). CXCL8 also binds to and activates another chemokine receptor, CXCR1 (Stillie *et al.*, 2009; receptor nomenclature follows Alexander *et al.*, 2013).

CXCR2 and CXCL8 are involved in a number of neutrophil-mediated diseases and blockade of CXCR2 using peptides or low MW compounds has proved promising in disease models *in vivo*. Several low MW CXCR2 inhibitors have also advanced to clinical trials (Phase I and Phase II) for inflammation-mediated lung diseases, including chronic obstructive pulmonary disease (COPD) and cystic fibrosis (CF) (Holz *et al.*, 2010; Lazaar *et al.*, 2011). COPD is one of the leading causes of morbidity and mortality in developed countries, characterized by progressive airflow obstruction caused by (i) fibrosis and narrowing of small airways and (ii) destruction of alveolar attachments (emphysema), which are mediated by neutrophils and lymphocytes (Barnes, 2000, 2004). Concentrations of CXCL8 in sputum and bronchoalveolar lavage (BAL) are higher in patients with COPD than healthy volunteers, which correlates with increased neutrophil accumulation (Keatings *et al.*, 1996; Yamamoto *et al.*, 1997; Aaron *et al.*, 2001; Tanino *et al.*, 2002; Woolhouse *et al.*, 2002). Several clinical studies show that SB656933, a low MW CXCR2 selective inhibitor, can effectively suppress ozone- and LPS-induced lung inflammation in healthy patients by significantly reducing sputum neutrophils (Busch-Petersen, 2006; Lazaar *et al.*, 2011; Aul *et al.*, 2012). SCH 527123, a dual CXCR1 and CXCR2 inhibitor, is also being evaluated in clinical trials for inflammation-mediated lung diseases. SCH 527123 had similar efficacy as SB656933 in LPS- and ozone-induced lung inflammation in healthy patients and also reduced sputum neutrophils and exacerbations in patients with severe asthma (Holz *et al.*, 2010; Aul *et al.*, 2012; Nair *et al.*, 2012). Additionally, these studies show that blockade of CXCR2 via SB656933 and SCH 527123 is safe and well tolerated in patients.

Although the therapeutic potential of CXCR2 blockade is well documented, there are fewer low MW antagonists of CXCR2, than of other clinically relevant molecular targets. Several distinct classes of CXCR2 blockers have been reported, which include diarylureas (SB225002, SB265610, SB656933), cyanoguanidine (SB468477), squaramides (SCH-527123), pyrimidines (AZ-10397767) and ketoprofen derivatives (Figure 1) (White *et al.*, 1998; Bertini *et al.*, 2004; Traves *et al.*, 2004; Hunt *et al.*, 2007; Chapman *et al.*, 2007). More recent studies show that many of these previously reported CXCR2 blockers behave as allosteric antagonists rather than competitive inhibitors. Using site-directed mutagenesis strategies, Salchow *et al.* (2010) demonstrated that SB265610 and SCH527123 both bind to CXCR2 at a common, allosteric, intracellular site, in close proximity to the site of G-protein coupling. Using similar techniques, Catusse *et al.* (2003) showed the N-terminus and second extracellular loop of CXCR2 is critical for ligand binding. Most importantly, these studies showed that the amino acid residues critical for activation were not involved in binding. This offers several insights to developing CXCR2 inhibitors. Firstly, as the activation site and the binding site are distinct, compounds designed to specifically target either one of these sites would be sufficient to partially or completely inhibit receptor activity. Secondly, using the conventional ligand competitive

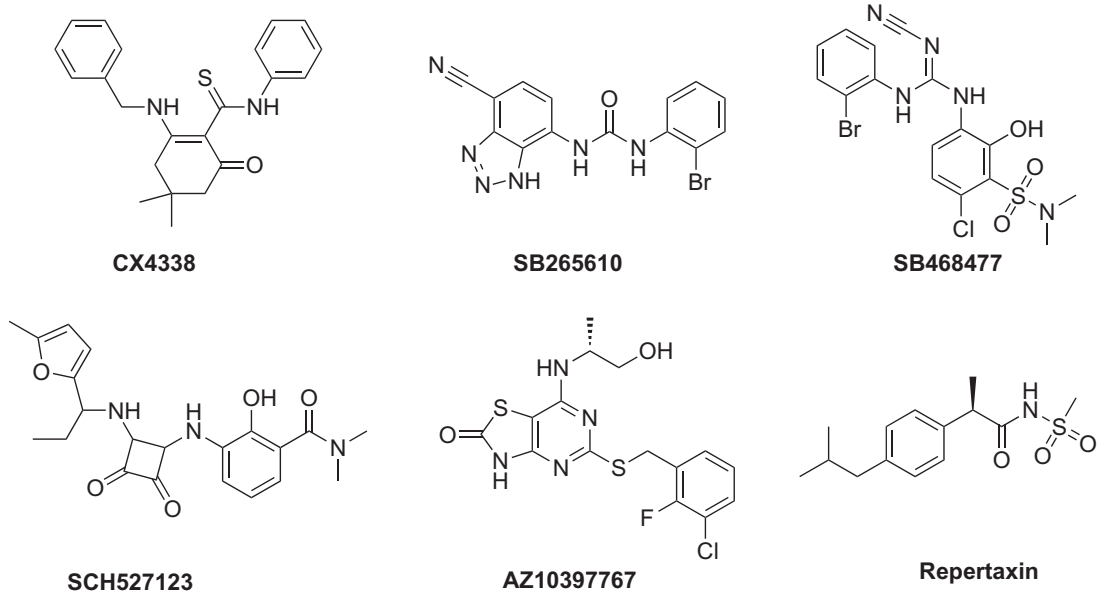

Figure 1

Chemical structures of CX4338 and previously reported CXCR2 antagonists (SB265610, SB468477, SCH527123, AZ10397767 and Repertaxin).

binding assay to screen for CXCR2 blockers limits the identification of compounds to those that target only the binding site. Thus, using an activation assay to perform initial screens may improve the rate of identification of potential new CXCR2 blockers.

Taking these insights into consideration, we used a cell-based reporter gene assay that detects CXCR2-mediated β-arrestin-2 recruitment upon receptor activation as our initial screening platform. A novel compound, CX4338 [2-(benzylamino)-4,4-dimethyl-6-oxo-*N*-phenylcyclohex-1-enecarbothioamide], was identified from our screening endeavours and further characterization of CX4338 led to elucidation of its mechanism of action on CXCR2. CX4338 blocks the effects of activated CXCR2 through selective inhibition of CXCR2/β-arrestin-2 signalling, which is sufficient to inhibit CXCL8-mediated chemotaxis and LPS-stimulated recruitment of neutrophils in mice.

Methods

Cell culture

Tango™ CXCR2-bla and CXCR4-bla U2OS cells were purchased from Invitrogen (Carlsbad, CA, USA) and grown in McCoy5A supplemented with 10% dialysed FBS, zeocin (200 μg·mL^{-1}), hygromycin (50 μg·mL^{-1}), geneticin (100 μg·mL^{-1}), 1 mM sodium pyruvate, 0.1 mM non-essential amino acids and 25 mM HEPES. HEK293 cells overexpressing HA-tagged CXCR2 and GFP-tagged β-arrestin-2 (HEK293-HA-CXCR2-β-arrestin-2-GFP) were kindly provided by Dr O. M. Zack Howard, NCI. These cells were grown in DMEM supplemented with 10% FBS and geneticin (800 μg·mL^{-1}) and puromycin (2 μg·mL^{-1}). 293T cells overexpressing GFP-tagged CXCR2 (293T-CXCR2-GFP) were stably generated by Dr Daryl Davies (University of Southern California, School of Pharmacy, Los Angeles, CA, USA) using a lentiviral system. 293T-CXCR2-GFP cells were cultured in DMEM (Invitrogen) supplemented with 10% FBS and puromycin (2 μg·mL^{-1}). To generate 293T-CXCR2-GFP-p22F cells, 293T-CXCR2-GFP cells were transfected with the pGlosensor-22F cAMP plasmid (Promega, Madison, WI, USA) using Lipofectamine 2000 (Invitrogen). 293T-CXCR2-GFP-p22F cells were cultured in DMEM supplemented with 10% FBS, puromycin (2 μg·mL^{-1}) and hygromycin B (200 μg·mL^{-1}). H1299, H460, Jurkat, HL60 and U2OS cells were purchased from American Type Culture Collection (ATCC, Manassas, VA, USA) and were grown in RPMI-1640 (Invitrogen) supplemented with 10% FBS. All cells were grown at 37°C in a humidified atmosphere of 5% CO_2. All cell lines used were maintained in culture under 35 passages and tested regularly for *mycoplasma* contamination using PlasmoTest™ (InvivoGen, San Diego, CA, USA).

Normal human airway epithelial cells (NuLi; ATCC) and CF human airway epithelial cells (CuFi; ATCC) were maintained in serum-free bronchial epithelial basal medium (Lonza, Walkersville, MD, USA) supplemented with BEGM SingleQuots (Lonza) without gentamicin and amphotericin B. Cells were cultured in flasks pre-coated with human placental collagen type IV (Sigma, St. Louis, MO, USA), maintained at 37°C in a humidified atmosphere (5% CO_2), fed every 48 h and passaged at 90–95% confluence. NuLi and CuFi cells were maintained in culture under 25 passages and tested regularly for *Mycoplasma* contamination using MycoAlert Mycoplasma Detection Kit™ (Lonza, Rockland, ME, USA).

CXCR2 and CXCR4 Tango assay

CXCR2-bla U2OS cells were genetically modified to stably overexpress CXCR2 linked to a TEV protease site and a GAL4-VP16 transcription factor. These cells also stably express a β-arrestin-2/TEV protease fusion protein and a β-lactamase reporter gene. Upon CXCL8 binding and CXCR2 activation, the β-arrestin-2/TEV fusion protein is recruited to the receptor and cleaves the peptide linker that links CXCR2 to the GAL4-VP16 transcription factor. GAL4-VP16 now can enter the nucleus and promote the transcription of the β-lactamase gene. β-Lactamase activity is detected using a FRET-based fluorescence assay with CCF4-AM, a β-lactamase FRET substrate. CCF4-AM is cleaved in the presence of β-lactamase. The cleaved substrate excites at 409 nm and emits at 447 nm. In the absence of β-lactamase, CCF4-AM will not be cleaved and excites at 409 nm and emits at 520 nm. Thus, CXCL8 activation of CXCR2 is directly correlated with the amount of cleaved β-lactamase substrate. In each assay, CXCR2 or CXCR4-bla U2OS cells were seeded (10 000 per well) in 384-well tissue culture plates for 24 h in DMEM supplemented with 1% FBS. Cells were pre-treated with various concentrations of inhibitors for 30 min prior to the addition of 20 nM of CXCL8 or 30 nM of CXCL12 and incubated for 5 h at 37°C. β-Lactamase substrate was loaded for 2 h and plates were read on Envision microplate reader (PerkinElmer, Waltham, MA, USA) at 405 nm excitation and 460/535 nm emissions. Percentage inhibition was calculated using the following formulas:

Ratio for each sample well:
cleaved (405/460)/uncleaved (405/535)

% Inhibition
= {1 – [(Compound treated – unstimulated control)/(CXCL8/CXCL12 stimulated – unstimulated control)]} × 100

CXCR2 in-cell Western assay

CXCR2-bla U2OS cells were grown in growth media (McCoy5A supplemented with 10% dialysed FBS) until 70–80% confluence was reached. Growth medium was removed and cells were washed with PBS. Cells were detached with 0.25% trypsin-EDTA for 5 min at 37°C. Trypsin was neutralized with 5 mL of growth media and cells were centrifuged at 161× *g* for 5 min at 37°C. Cells were seeded (11 000 cells per well) in 384-well tissue culture plates in 40 μL of assay media (DMEM supplemented with 1% FBS) and incubated at 37°C overnight. The next morning, the assay medium was removed and cells were pre-treated with various concentrations of SB265610 or CX4338 (36 μL total volume) for 30 min. Four microlitres of 10X CXCL8 was added to each well. For receptor internalization, plates were incubated with CXCL8 for 30 min. To detect total CXCR2, plates were incubated with CXCL8 for 5 h at 37°C. Compounds and CXCL8 were removed and cells were fixed with 4% formaldehyde (25 μL per well) for 20–30 min at room temperature.

Formaldehyde was removed and wells were washed with PBS and stored at 4°C. The next day, each well was blocked in blocking buffer (Li-Cor, Lincoln, NE, USA) for 2 h at room temperature and incubated with CXCR2 antibodies (1:1000 dilution in blocking buffer; Santa Cruz Biotechnology, Santa Cruz, CA, USA) for 2 h at room temperature or overnight at 4°C. Cells were then washed with PBS six times and incubated with mouse IRDye 680RD secondary antibodies (1:1000 dilution in blocking buffer, 25 µL per well) for 1 h in the dark. Wells were washed with PBS six times. Plates were centrifuged upside down on top of paper towels at 161× *g* for 5 min to remove excess liquid. Plates were allowed to completely dry before imaging and quantification on the Li-Cor Odyssey bioimager. To detect total CXCR2 (receptor degradation), cells were blocked in blocking buffer with 0.3% Triton X-100 (Fisher Scientific, Pittsburgh, PA, USA) for 2 h. Primary and secondary antibodies were also diluted in 0.3% Triton X-100 in blocking buffer. Percentage inhibition of receptor internalization and degradation was calculated using the following formula:

$$\%\ \text{Inhibition} = [(\text{Compound treated} - \text{CXCL8 stimulated})/(\text{unstimulated control} - \text{CXCL8 stimulation})] \times 100$$

Cyclic AMP assay

293T-CXCR2-GFP-p22F cells were seeded in CO_2-independent media (Invitrogen) supplemented with 10% FBS at 30 000 cells per well overnight in white 384-well plates. Cells were incubated with 1% cAMP reagent (Promega) for 2 h at 37°C the following day. Cells were pre-treated with various concentrations of CX4338 or SB265610 for 10 min, then stimulated with CXCL8 (50 nM) for additional 10 min, and forskolin (50 µM) stimulation until maximum cAMP signal was reached (10–20 min). In longer time point studies, cells were pre-treated with CX4338 for 1 h prior to stimulation with CXCL8 (50 nM) and forskolin (50 µM). Luminescence signals were detected using the Envision microplate reader (PerkinElmer). Percentage inhibition was calculated using the following formula:

$$\%\ \text{Inhibition} = [(\text{Compound/CXCL8/Forskolin} - \text{Forskolin/CXCL8})/(\text{Forskolin only} - \text{Forskolin/CXCL8})] \times 100$$

Neutrophil chemotaxis

Blood was collected from healthy human volunteers for neutrophil isolation. All experiments were conducted with the approval of the University of Southern California Institutional Review Board. Blood was collected into EDTA-sprayed tubes (Greiner Bio-One, Monroe, NC, USA), and neutrophils were isolated using One-Step Polymorph separation media (Accurate Chemical and Scientific, Westbury, NY, USA) with centrifugation at 500× *g* for 35 min, according to the manufacturer's recommendations. RBC lysis buffer (IBI Scientific, Peosta, IA, USA) was used to remove residual erythrocytes. The final pellet of neutrophils was resuspended in HBSS without Ca^{2+} or Mg^{2+} (Lonza) supplemented with 1% BSA (Amresco, Solon, OH, USA) and kept on ice. Neutrophils were counted using Turk's blood diluting fluid (Ricca Chemical, Arlington, TX, USA) and a haemocytometer. Viability was assessed by Trypan blue exclusion. All preparations consisted of approximately 95% viable neutrophils.

Neutrophils were incubated in triplicate with a range of concentrations of CX4338 or vehicle (1% DMSO) for 1 h. Neutrophils were then placed in the top wells of a 96-well MultiScreen-MIC plate with 3 µm pore size (Millipore, Billerica, MA, USA) containing 50 nM of CXCL8 in the bottom wells. Neutrophils were allowed to migrate for 2–4 h at 37°C and 5% CO_2. In some experiments, the migrated neutrophils in the bottom wells were stained with Turk's blood diluting fluid and manually counted with a haemocytometer. In other experiments, the migrated neutrophils were labelled with CyQuant NF dye (Invitrogen, Eugene, OR, USA), and fluorescence intensity was measured using a spectrofluorometer with excitation at 485 nm and emission at 530 nm (PerkinElmer). Neutrophil count was calculated using a standard curve. Percentage of maximal chemotaxis was calculated using the following formula:

$$\%\ \text{Maximal chemotaxis} = [(\text{number of treated cells migrated with CXCL8} - \text{number of untreated cells migrated without CXCL8})/(\text{number of untreated cells migrated with CXCL8} - \text{number of untreated cells migrated without CXCL8})] \times 100$$

Data were plotted using a sigmoidal E_{max} model to estimate IC_{50}, the concentration associated with a 50% inhibition of the maximal chemotactic response.

LPS-induced lung inflammation

All animal care and experimental procedures were approved by the University of Southern California Institutional Animal Care and Use Committee (Protocol No. 11675). All studies involving animals are reported in accordance with the ARRIVE guidelines for reporting experiments involving animals (Kilkenny *et al.*, 2010; McGrath *et al.*, 2010). A total of 9 animals were used in the experiments described here.

Eight- to ten-week-old male BALB/c mice were obtained from Charles River Laboratories (Hollister, CA, USA) and were maintained in the animal facilities at Zilkha Neurogenetic Institute (Los Angeles, CA, USA). Three experimental groups with three animals in each group (LPS vehicle; LPS+CX4338; LPS+ SB265610) at 24 h were used for pharmacodynamics evaluation of LPS-induced airway inflammation. Animals had access to food and water and were kept in controlled laboratory conditions with an average temperature of 71°F and a light–dark cycle of 12 h. A single 1 mL injection containing CXCR2 antagonists (CX4338, SB265610) diluted in 5% DMSO in normal saline or vehicle only (5% DMSO in normal saline) was administered s.c. 30 min prior to LPS insufflation. All compounds were aseptically prepared and sterile-filtered through a 0.22 µm filter. Acute lung inflammation was induced by intranasal LPS insufflation (1 µg/20 g body weight) under light sedation [100 µL of a ketamine (80 mg·kg^{-1}) and xylazine (10 mg·kg^{-1}) solution]. At 24 h, airway leukocytes were collected by bronchoscopy. BAL was performed after lethal i.p. administration of Euthasol (75 mg·kg^{-1}). The trachea was exposed through a midline incision with subsequent insertion of a 26 G tracheal tube.

The lungs were washed three times with three different aliquots of PBS (1, 0.8 and 0.8 mL) with recovery via syringe aspiration of 86%. BAL samples were placed on ice and centrifuged at 360× *g* and 4°C for 10 min. The cell pellet was used to evaluate the number of infiltrating leukocytes. Total and differential airway cell counts were determined for each BAL sample using a haemocytometer and Wright stain to examine nuclear morphology under the microscope.

Data analysis

Statistical and graphical analysis was carried out using GraphPad Prism version 5.04 (GraphPad Software, San Diego, CA, USA) and Microsoft Excel 2010. *P*-values were calculated using unpaired Student's *t*-test.

Materials

Compounds were prepared as 10 mM stock solutions in DMSO and stored at –20°C. All compounds were purchased from Asinex (Moscow, Russia) and Enamine (Kiev, Ukraine). SB265610 was purchased from Tocris Bioscience (Ellisville, MI, USA). Human CXCL8 cDNA was inserted into the expression vector, pET32a, at EcoR1 and XhoI restriction sites to generate His-tagged CXCL8. The sequence of the clone was confirmed by DNA sequencing. The CXCL12α (SDF-1α) expression vector was kindly provided by Dr. Ghalib Alkhatib. Recombinant CXCL8 and CXCL12α were expressed in BL21-Gold (DE3) pLysS strain of *Escherichia coli* (Stratagene, La Jolla, CA, USA) and purified using a previously reported protocol (Altenburg *et al.*, 2007).

Results

Identification of CX4338

The binding of CXCL8 to CXCR2 triggers desensitization, a process mediated by the recruitment of β-arrestin1/2 to the activated receptor, which may be detected by monitoring the coupling of β-arrestin1/2 and CXCR2 (Barlic *et al.*, 1999; Yang *et al.*, 1999; Richardson *et al.*, 2003; Raghuwanshi *et al.*, 2012). This interaction can be monitored using the CXCR2 Tango assay, which is a cell-based reporter gene assay, as described in the Methods. Using this assay, we screened 2000 compounds from an in-house library of highly diverse compounds. To test for receptor specificity, we also used the CXCR4 Tango assay to counter-screen compounds that show activity on CXCR2. CXCR4 belongs to the same family of chemokine receptors as CXCR2 but is activated by another chemokine, CXCL12.

From our screening process, we identified several different classes of compounds that show activity on CXCR2 with IC_{50} values between 500 nM and 50 μM (Supporting Information Table S1 and Fig. S1). From this set of compounds, CX4338 was chosen for further mechanistic studies due to its specificity for CXCR2 and lack of cytotoxic effects on several CXCR2-expressing cell lines (Figures 1 and 2A). CX4338 inhibited CXCR2-mediated β-arrestin-2 recruitment with an IC_{50} of 6.3 μM, while showing little to no inhibition of CXCR4-mediated β-arrestin-2 recruitment (IC_{50} > 100 μM; Figure 2B and Table 1). At concentrations as high as 50 and 100 μM, CX4338 did not decrease cell viability in several CXCR2-expressing cell lines (Table 2 and Supporting Information Fig. S2). As the chemical structure of CX4338 is distinct from the previously reported CXCR2 antagonists (Figure 1), we sought to compare CX4338 with a well-characterized CXCR2 antagonist, SB265610. In the Tango assay, SB265610 inhibited CXCR2-mediated β-arrestin-2 recruitment with an IC_{50} of 0.28 μM (Figure 2A, Table 1). Further, upon CXCL8 stimulation, β-arrestin-2 is rearranged into vesicles (represented as punctate staining) in HEK293 cells overexpressing CXCR2 and GFP-tagged β-arrestin-2 (Figure 3). In the presence of CX4338 (50 μM) or SB265610 (5 μM), β-arrestin-2 rearrangement was inhibited and no punctate staining was observed (Figure 3).

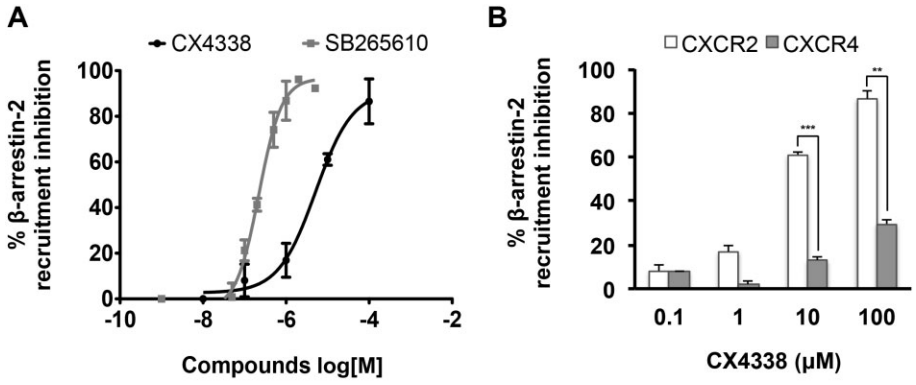

Figure 2

CX4338 selectively inhibits CXCR2-mediated β-arrestin-2 recruitment. (A) Concentration-inhibition curve of CX4338 and SB265610 in the CXCR2 Tango™ assay. CXCR2-bla U2OS cells were pre-treated with indicated concentrations of CX4338 or SB265610 for 30 min. Cells were then stimulated with 20 nM of CXCL8 for 5 h. Cells were loaded with a β-lactamase substrate for 2 h and the amount of cleaved and uncleaved substrate was measured using the Envision plate reader (excitation at 405 nm and emissions at 460 and 535 nm). Data represent mean ± SEM of three to nine independent experiments. (B) CX4338 selectively inhibits CXCR2 over CXCR4. CXCR2-bla or CXCR4-bla U2OS cells were pre-treated with CX4338 for 30 min before stimulation with 20 nM of CXCL8 or 30 nM of CXCL12 for 5 h. Data represent mean ± SEM of three to nine independent experiments. $^{**}P < 0.001$, $^{***}P < 0.0001$; Student's *t*-test.

Table 1

IC_{50} values for CXCR2 and CXCR4 inhibition

Compound	CXCR2 (IC_{50}, μM)[a]	CXCR4 (IC_{50}, μM)[a]	Selectivity[b]
SB265610	0.28 ± 0.09	>20	>71.4
CX4338	6.3 ± 1.3	>100	>15.9

[a]IC_{50} = concentration required to inhibit 50% of CXCR2 or CXCR4 in the Tango™ assay.
[b]Selectivity was calculated by dividing the IC_{50} value for CXCR4 by that for CXCR2. Data are presented as mean ± SD of three independent experiments.

Table 2

Percentage cell viability upon CX4338 treatment

Cell lines	% Cell viability at 100 μM	% Cell viability at 50 μM
CXCR2-bla U2OS[a]	86.0 ± 3.3	NT
CXCR4-bla U2OS[a]	97.8 ± 9.4	NT
293T-CXCR2[a]	75	NT
293T[a]	90.8	NT
H460[a]	86.4 ± 11.4	NT
H1299[a]	107 ± 5.1	NT
U2OS[a]	97	NT
Jurkat[b]	NT	89.1 ± 9.8
HL60[b]	NT	74.6 ± 25.4
NuLi[c]	102 ± 3.4	NT
CuFi[c]	117 ± 7.4	NT

Data are presented as mean ± SD of one to four independent experiments.
[a]Cells were treated with CX4338 for 72 h and cell viability assessed with MTT assay.
[b]Cells were treated with CX4338 for 72 h and cell viability was assessed with AlamarBlue assay.
[c]Cells were treated with CX4338 for 24 h and cell viability was assessed with MTT assay.
NT, not tested.

CX4338 inhibits receptor internalization

Upon β-arrestin1/2 recruitment during CXCL8 stimulation, CXCR2 is internalized via clathrin-mediated endocytosis and routed for cell surface recycling or to late endosomes/lysosomes for receptor degradation (Yang *et al.*, 1999; Fan *et al.*, 2003). To assess surface CXCR2 expression, we performed a high-throughput in-cell Western assay. When CXCR2-bla U2OS cells were treated with a range of CXCL8 concentrations (1–100 nM) for various time points, CXCL8 induced CXCR2 receptor internalization in a time- and concentration-dependent manner. We observed up to 60% CXCR2 internalization as early as 5 min when cells were stimulated with 100 nM of CXCL8 (Supporting Information Fig. S3). To assess the effects of CX4338 and SB265610 on CXCL8-induced receptor internalization, CXCR2-bla U2OS cells were pre-treated with CX4338 at various concentrations for 30 min before CXCL8 stimulation (Figure 4A). In this assay, CXCL8 significantly stimulated receptor internalization as indicated by a significant decrease (56.7%) in cell surface CXCR2 expression within 30 min of stimulation (Figure 4B). Pre-treatment with 50 and 20 μM of CX4338 inhibited CXCL8-induced receptor internalization by ~70% (Figure 4C). SB265610 was more potent than CX4338 at inhibiting CXCL8-induced receptor internalization. For example, 5 μM of SB265610 inhibited CXCL8-induced receptor internalization by 88%, whereas 5 μM of CX4338 inhibited receptor internalization by 20% (Figure 4C).

Next, we also assessed total CXCR2 using a similar in-cell Western assay. However, prior to CXCR2 detection, cells were permeabilized to detect both surface and intracellular CXCR2. CXCL8 also reduced total CXCR2 expression (by mediating receptor degradation) in a concentration-dependent manner (Supporting Information Fig. S4). CXCR2 stimulation with 50 nM of CXCL8 reduced total CXCR2 expression by 22.5% within 5 h of incubation (Figure 4D,E). Pre-treatment with CX4338 did not inhibit the effects of CXCL8 on total CXCR2 (Figure 4F). However, SB265610 potently inhibited the effects of CXCL8 on total CXCR2, with greater than 100% inhibition at concentrations as low as 1 μM. Greater than 100% inhibition was observed with SB265610 because it behaves as an inverse agonist.

CX4338 enhances CXCR2-mediated G-protein signalling

Two main signalling cascades mediate CXCR2 signalling: β-arrestin1/2 coupling and $G_{\alpha}i$-protein signalling mediated by second messengers, such as calcium, kinases and cAMP (Hall *et al.*, 1999; Fan *et al.*, 2001; Su *et al.*, 2005). Since we showed that CX4338 inhibited CXCR2-mediated β-arrestin-2 recruitment, rearrangement and receptor internalization, we postulated that CX4338 would also inhibit CXCR2-mediated G_i-protein signalling. Thus, we also assessed the effects of CX4338 on calcium mobilization, MAPK phosphorylation and cAMP signalling.

CXCL8 rapidly induced calcium mobilization in 293T-CXCR2-GFP cells, reaching a peak within 30 s. Co-treatment with SB265610 at 5 and 2 μM and CXCL8 reduced CXCL8-mediated calcium mobilization (Figure 5A). However, co-treatment with CX4338 and CXCL8 enhanced calcium mobilization, sustaining peak calcium release up to 60 s and increased basal calcium release (Figure 5B). Cells pre-treated with SB265610 for 12 min before stimulation with CXCL8 show that SB265610 alone initially increased basal calcium levels. However, upon CXCL8 stimulation, pre-treatment with SB265610 completely inhibited CXCL8-mediated calcium mobilization (Figure 5C). CX4338 alone induced a slow and steady increase in intracellular calcium levels and pre-treatment with CX4338 for 12 min did not enhance peak calcium release induced by CXCL8, compared with DMSO pre-treated cells (Figure 5D). SB265610 and CX4338-induced calcium release may be due to non-specific effects of the compounds at high concentrations. Thus, the enhanced calcium release observed when cells were co-treated with CX4338 and CXCL8 may be due to non-specific effects. It is also important to note that CX4338-induced calcium release may also be a CXCR2-mediated event, which may occur due

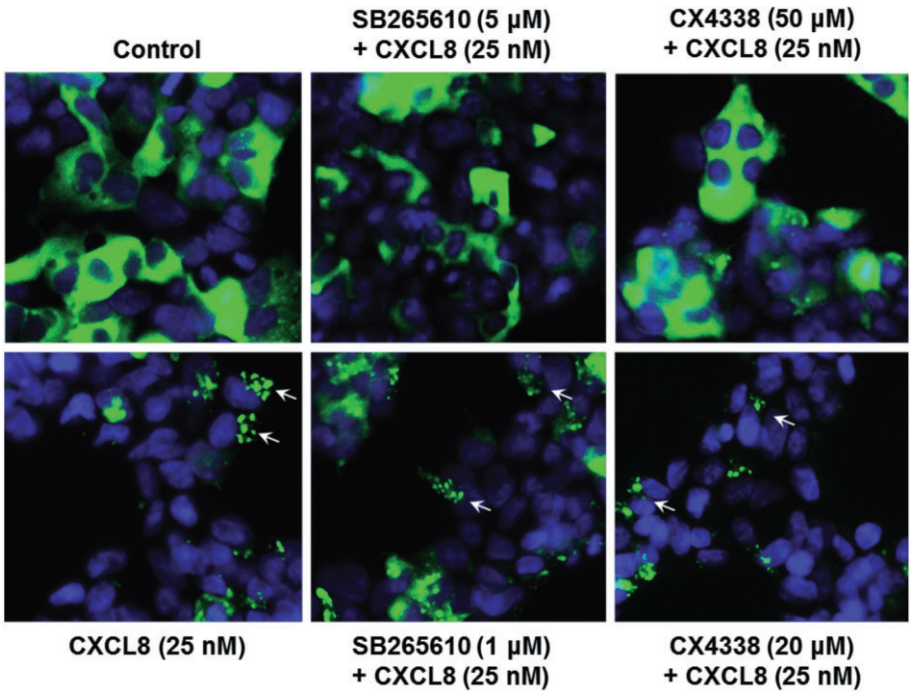

Figure 3

CX4338 inhibits β-arrestin-2 rearrangement. HEK293-CXCR2-β-arrestin-2-GFP cells were seeded at 10 000 cells per well in a 384-well black, clear bottom plate in 32 μL of growth media overnight. Cells were pre-treated with 50 and 20 μM of CX4338 or 5 and 1 μM of SB265610 for 30 min prior to stimulation with 25 nM of CXCL8 for an additional 30 min at 37°C. Cells were fixed with 8% formaldehyde for 20 min, stained with the nuclear stain DAPI, and washed with PBS. Cells were imaged with the GFP and DAPI filter on the BD Pathway. DAPI staining is represented in blue and GFP is represented in green. The white arrows indicate punctate staining.

the selective inhibition of the CXCR2/β-arrestin-2 pathway and subsequent up-regulation of CXCR2/G-protein-mediated signalling.

Cells stimulated with CXCL8 transiently induce ERK1/2 phosphorylation, which is believed to be primarily mediated by G-protein signalling (Nasser *et al.*, 2007; 2009). Consistent with previous studies, CXCL8 increased ERK1/2 phosphorylation, whereas pre-treatment with SB265610 at 5 μM completely inhibited ERK1/2 phosphorylation (Figure 6A). However, 30 min pre-treatment with CX4338 at 50 μM markedly enhanced CXCL8-induced ERK1/2 phosphorylation within 5 min and sustained this effect up to 10 min (Figure 6B). CX4338 without CXCL8 stimulation did not induce ERK1/2 phosphorylation. Previous studies showed that enhanced CXCR2-mediated G-protein signalling in β-arrestin1/2-deficient cells led to activation of stress kinases (Zhao *et al.*, 2004), thus, we also assessed the effects of CX4338 on p38 and JNK activation. CX4338 alone slightly induced JNK and p38 phosphorylation (Figure 6B). Pre-treatment with CX4338 before CXCL8 stimulation for 5 min also enhanced JNK phosphorylation compared with DMSO pre-treated cells (Figure 6B). CXCL8 did not induce p38 phosphorylation in DMSO pre-treated control cells. Pre-treatment with CX4338 before CXCL8 stimulation did not noticeably increase p38 activation as well (Figure 6B).

Next, we assessed the effects of CX4338 on CXCL8-mediated cAMP signalling. CXCR2 is coupled to the $G\alpha_i$-protein, which is a negative regulator of adenylyl cyclase (the enzyme that converts ATP to cAMP). We used a high-throughput cell-based assay employing the Glosensor™ technology (luciferase-based) to detect cAMP levels induced by forskolin (activator of adenylyl cyclase). CXCL8 significantly reduced forskolin-stimulated cAMP production (Supporting Information Fig. S5). SB265610 dose-dependently inhibited the effects of CXCL8 on forskolin-stimulated cAMP production (IC_{50} =3.8 μM; Figure 7A,B), whereas CX4338 did not have any effects on CXCL8-mediated cAMP signalling at the range of concentrations tested (Figure 7C). We also increased the pre-treatment time of CX4338 from 10 min to 1 h before CXCL8 and forskolin stimulation and did not observe any significant effects on CXCL8-mediated cAMP signalling (Figure 7D).

CX4338 inhibits CXCL8-mediated chemotaxis

After we assessed the effects of CX4338 on CXCR2-mediated signalling, we next assessed the cellular effects of CX4338. CXCL8 is a potent chemoattractant that mediates the chemotaxis of neutrophils and endothelial cells during infection and angiogenesis. CXCL8 markedly induced cell migration in both wound healing and transwell cell migration assays in CXCR2-overexpressing cells (Figure 8A,B). CX4338 and SB265610 dose-dependently inhibited CXCL8-mediated cell migration in a wound healing assay (Figure 8A). Both CX4338 and SB265610 abolished cell migration at 10 μM. CX4338 also completely inhibited cell migration using

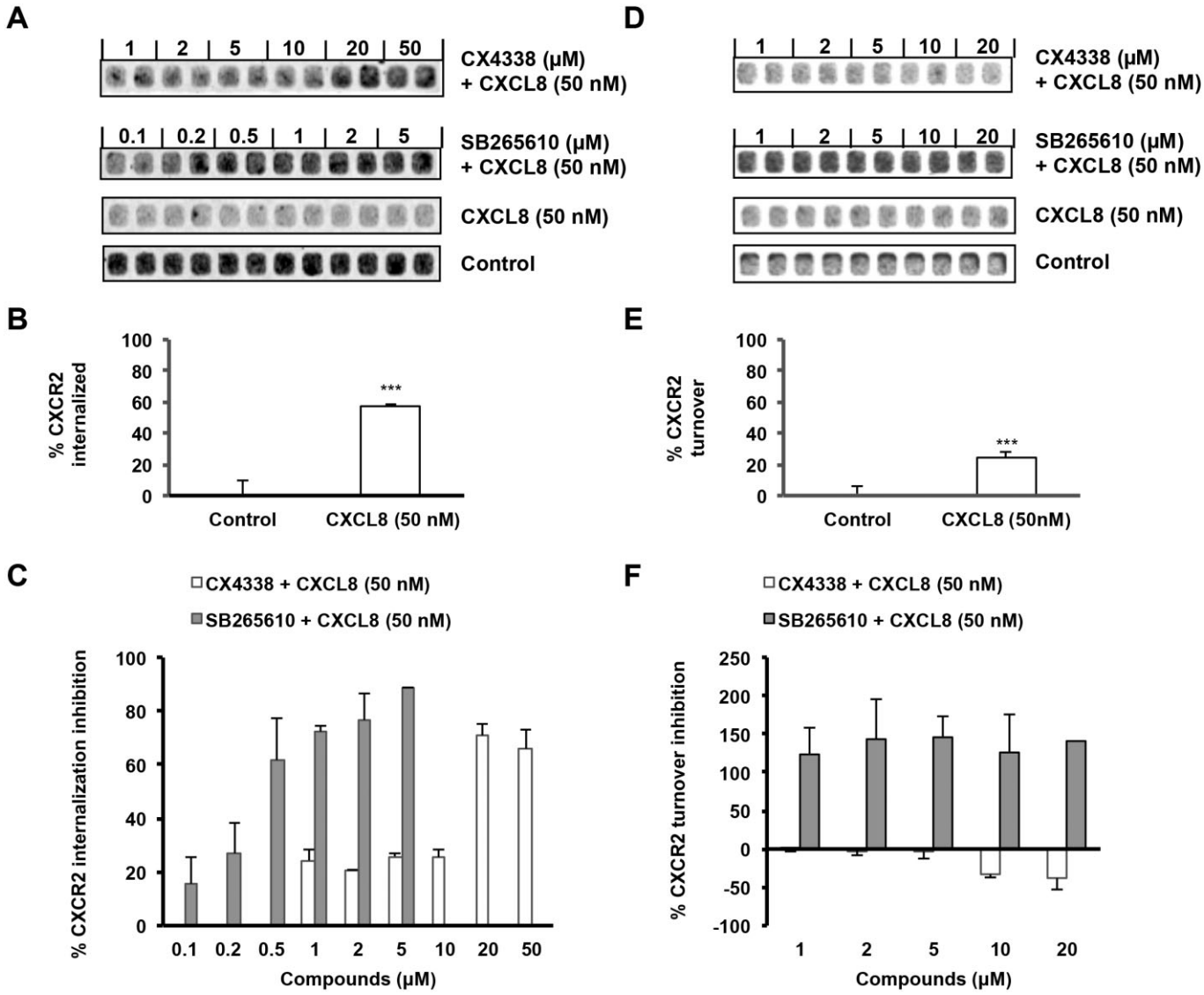

Figure 4

CX4338 inhibits CXCL8-mediated CXCR2 internalization. (A) CX4338 and SB265610 concentration-dependently inhibit CXCL8-mediated CXCR2 internalization. Cells were pre-treated with CX4338 or SB265610 at indicated concentrations for 30 min prior to stimulation with 50 nM of CXCL8 for an additional 30 min. (B) Quantification of (A) showing percentage CXCR2 internalized induced by 50 nM of CXCL8. Data is normalized to unstimulated control and represents mean ± SD of a representative experiment ($n = 12$). ***$P < 0.0001$; Student's *t*-test. (C) Pre-treatment with CX4338 and SB265610 concentration-dependently inhibited CXCL8-induced receptor internalization (same treatment as A). Data represent mean ± SD of two independent experiments. (D) CX4338 does not inhibit CXCL8-mediated CXCR2 turnover. Cells were pre-treated with CX4338 or SB265610 at indicated concentrations for 30 min before stimulation with 50 nM of CXCL8 for 5 h. (E) Quantification of (D) showing percentage CXCR2 turnover induced by 50 nM of CXCL8. Data are normalized to unstimulated control and represents mean ± SD of a representative experiment ($n = 10$). ***$P < 0.0001$; Student's *t*-test. (F) Quantification of images shown in (D). CX4338 did not inhibit CXCL8-mediated receptor turnover, but rather slightly enhanced receptor turnover. SB265610 inhibited CXCL8-mediated receptor turnover above 100%, acting as an inverse agonist. Data represent mean ± SD of at least two independent experiments performed in duplicate.

transwell inserts, at concentrations as low as 1 μM (Figure 8B). SB265610 was not tested.

CX4338 inhibits polymorphonuclear leukocytes (PMNs) migration in LPS-induced inflammation model

The anti-chemotactic effects of CX4338 on PMNs neutrophils were investigated in *in vitro* and *in vivo* models. *In vitro* testing using a modified Boyden chamber transwell assay measured human neutrophils chemotaxis towards 50 nM of CXCL8. We previously determined that 50 nM of CXCL8 was an optimal concentration to induce chemotaxis (data not shown). As shown in Figure 9A, CX4338 inhibited CXCL8-induced chemotaxis in a concentration-dependent manner, with an IC_{50} of 68.6 μM (Supporting Information Fig. S6). More importantly, 5 mg·kg^{-1} of CX4338 was also able to

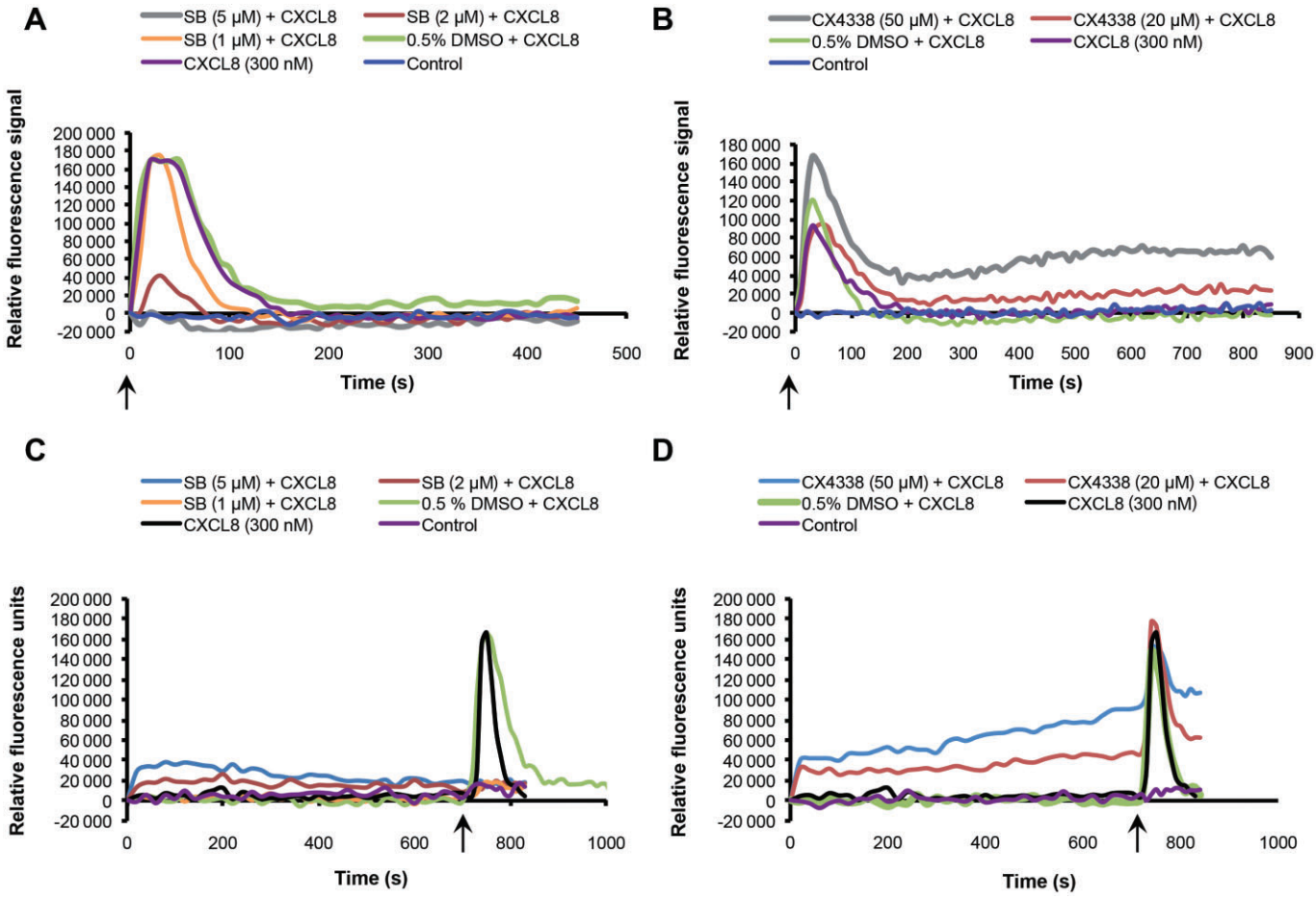

Figure 5

CX4338 enhances CXCL8-induced calcium release. (A) SB265610 inhibits CXCL8-induced calcium mobilization. 293T-CXCR2-GFP cells were seeded at 30 000 cells per well in 384-well black/clear bottom plates in complete media overnight. Cells were loaded with Fluo-4 NW dye and 2.5 mM of probenecid and incubated at 37°C for 30 min and at room temperature for an additional 30 min. Cells were co-stimulated with various concentrations of SB265610 and 300 nM of CXCL8. Intracellular calcium flux was immediately read on the Envision plate reader at 495/535 nm. Cells were also co-stimulated with 0.5% DMSO and 300 nM of CXCL8. Control cells were not stimulated. (B) Cells were prepared as in (A) and co-stimulated with 300 nM of CXCL8 and CX4338 at indicated concentrations. Cells were also co-stimulated with 0.5% DMSO and 300 nM of CXCL8. Control cells were not stimulated. (C, D) Cells were pre-treated with SB265610, CX4338 or 0.5% DMSO for 12 min before CXCL8 (300 nM) stimulation. Relative fluorescence unit was normalized to basal signal. Arrows indicates time of CXCL8 stimulation.

significantly inhibit PMN migration (approximately 60% inhibition) in a murine model of neutrophilic airway inflammation induced by LPS (Figure 9B). Interestingly, 3 $mg \cdot kg^{-1}$ of SB265610 had similar effects on PMN migration.

Discussion and conclusions

Blockade of CXCR2 offers a promising therapeutic approach for a number of different inflammation-mediated diseases, including cancer, COPD, CF, asthma, psoriasis and arthritis (Suratt *et al.*, 2004; Traves *et al.*, 2004; Hristov *et al.*, 2007; Chapman *et al.*, 2009; Jacobs *et al.*, 2010). Using a high-throughput cell-based screening assay (Tango), we identified a novel thioamide compound, CX4338. This compound is structurally different from any reported CXCR2 blocker and has not been reported for any other molecular targets (Figure 1). While performing similarity searches for CX4338 within our in-house database of compounds, we found a similar compound, CX1142 (Supporting Information Fig. S1). Removing the thioamide from CX4338 and replacing it with a ketone increased its IC_{50} from 6.5 to 32 μM in the CXCR2 Tango assay (Table 1 and Supporting Information Table S1). It also markedly reduced its specificity for CXCR2, suggesting that the thioamide backbone structure is essential for anti-CXCR2 activity as well as specificity. Additional optimizations of CX4338 and structure activity relationship analysis may be able to significantly improve the potency and selectivity of CX4338 and further elucidate essential chemical features.

We postulate that CX4338 and SB265610 interact differently with CXCR2, as CX4338 and SB265610 belong to distinct chemical classes and regulate intracellular receptor signalling differentially, as observed with cAMP and ERK1/2

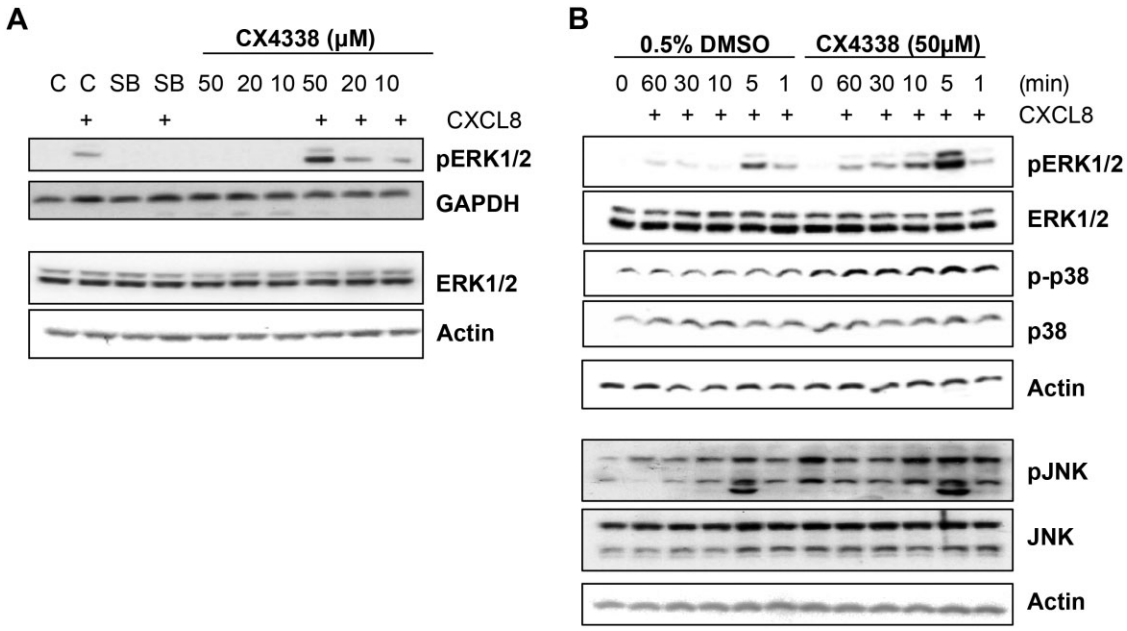

Figure 6

CX4338 enhances ERK1/2, p38 and JNK phosphorylation. (A) CX4338 enhanced ERK1/2 phosphorylation. 293T-CXCR2-GFP cells were seeded in 6-well plates at 500 000 cells per well for 5 h in complete media (DMEM supplemented with 10% FBS) and serum-starved (DMEM) overnight. Cells were pre-treated with CX4338 (50, 20, 10 μM) or SB265610 (SB, 5 μM) for 30 min and stimulated with CXCL8 (20 nM) for five minutes. ERK1/2 phosphorylation was detected using Western blot. Lanes indicated with 'C' are control lanes for untreated and CXCL8-stimulated cells. GAPDH and actin was used as a loading control. Data shown are a representative blot from two independent experiments. (B) CX4338 enhanced CXCL8-mediated MAP kinase signalling (p38, JNK and ERK1/2). Serum starved 293T-CXCR2-GFP cells were pre-treated with CX4338 (50 μM) or 0.5% DMSO for 30 min prior to CXCL8 (20 nM) stimulation at the indicated times.

phosphorylation. SB265610 acts as an allosteric, inverse agonist via binding to a common intracellular region of CXCR2 involving the C-terminus and intracellular loop 1 (Bradley *et al.*, 2009; Salchow *et al.*, 2010). Although a common intracellular allosteric site exists, studies with radiolabelled SB265610 and other CXCR2 antagonists suggest that distinct classes of antagonists exhibit different modes of binding to CXCR2, which is evidence of multiple allosteric sites (de Kruijf *et al.*, 2009, 2011). Additionally, acting as an inverse agonist, SB265610 inhibited CXCL8-mediated receptor degradation more than 100%, whereas CX4338 had little to no effect on receptor degradation (Figure 4). This suggests that CX4338 most likely does not act as an inverse agonist by locking CXCR2 in the inactive state. It is more likely that CX4338 interacts with CXCR2 on the C-terminus region near the receptor phosphorylation sites, which is critical for β-arrestin1/2 recruitment and receptor internalization. Interaction at this site may not necessarily shut down the entire receptor and still allow CXCR2 to mediate G-protein signalling. Also, consistent with our proposal that CX4338 may act as a non-competitive allosteric inhibitor, our preliminary results from Schild assays with the CXCR2 Tango method show that CX4338 has a Schild slope of 1.48 (Supporting Information Fig. S7 and Table S2). Since true competitive inhibitors have Schild slopes of 1, this suggests that CX4338 most likely does not act as an competitive antagonist at CXCR2 (Schild, 1947).

Mechanistic studies also suggested that CX4338 regulated CXCR2 function as a biased ligand, a mechanism that has not been previously observed with CXCR2 blockers. Both SB265610 and CX4338 inhibited CXCR2 β-arrestin-2 recruitment and subsequently inhibited receptor internalization (Figures 2–4). However, CX4338 enhanced ERK1/2 and JNK phosphorylation, whereas SB265610 potently inhibited all G-protein signalling (Figures 5–7). Generally, most GPCRs are regulated through G-protein and β-arrestin1/2 signalling, and it was thought that agonists or antagonists equally activate or inhibit all receptor-mediated signalling (referred to as correlated efficacies) (Reiter *et al.*, 2012). More recently, a number of biased ligands that selectively alter GPCR-mediated signalling have been reported for some GPCRs (see Rajagopal *et al.*, 2010b). Although biased ligands for CXCR2 have not been reported, biased ligands for other chemokine receptors (CXCR4 and CXCR7) have been described (Balabanian *et al.*, 2005; Rajagopal *et al.*, 2010a).

Biased inhibition of CXCR2/β-arrestin-2 signalling via CX4338 is consistent with previous findings. Neutrophils derived from β-arrestin-2 knockout mice and RBL-2H3 cells expressing phosphorylation-deficient CXCR2 demonstrated reduced CXCR2-mediated β-arrestin-2 translocation, receptor internalization and chemotaxis (Richardson *et al.*, 2003; Su *et al.*, 2005). Indirect β-arrestin1/2 inhibition via the deletion of G-protein receptor kinase 6 (GRK6), the kinase that mediates CXCR2 phosphorylation and subsequent β-arrestin1/2 recruitment, also showed decreased receptor internalization and chemotaxis (Raghuwanshi *et al.*, 2012). As β-arrestin1/2 is essential for receptor desensitization and negatively regulates G-protein signalling, enhanced CXCR2-mediated

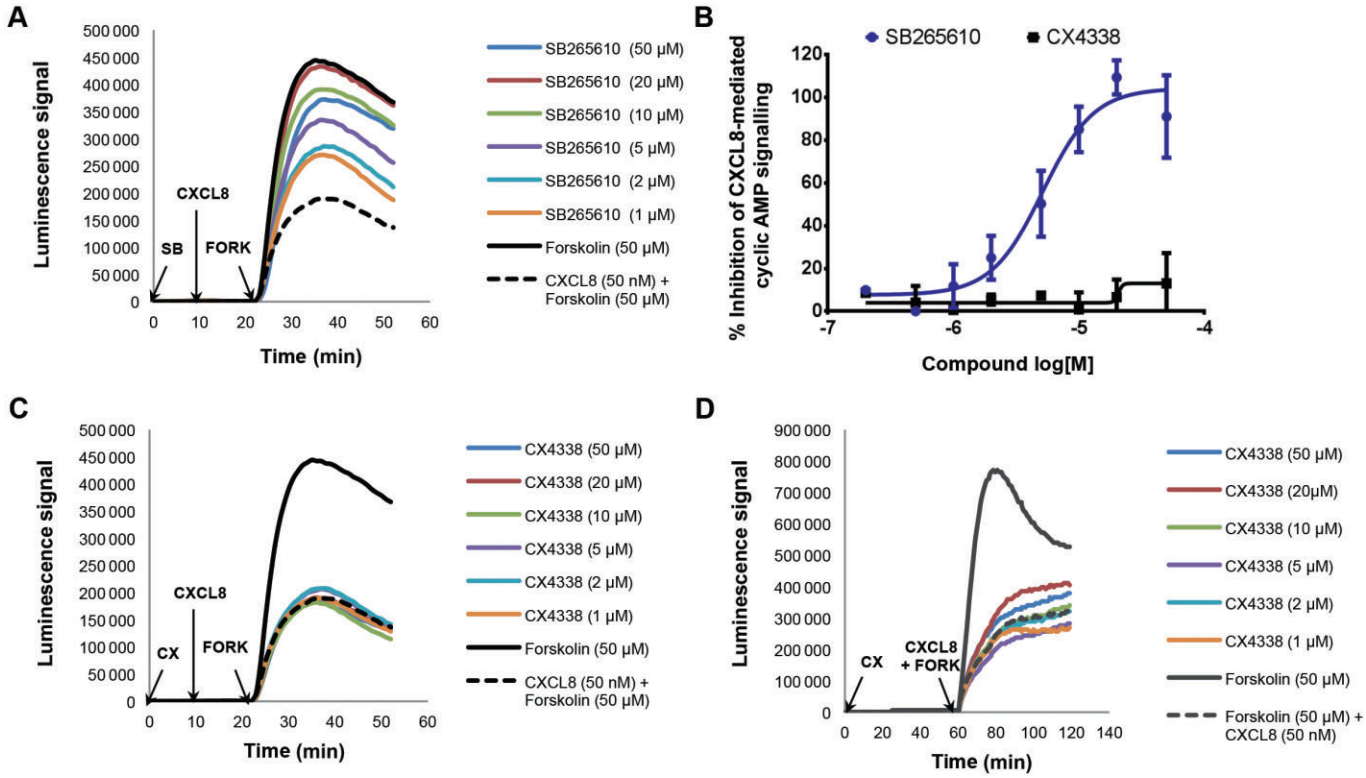

Figure 7

CX4338 does not alter CXCL8-mediated cAMP signalling. 293T-CXCR2-GFP-p22F cells were seeded at 30 000 cells per well in 384-well white plates in assay media (CO_2-independent media supplemented with 10% FBS). The next day, media was removed and cells were loaded with 1% cAMP reagent (Promega) diluted in assay media for two hours at room temperature (in the dark). Cells were pre-treated with (A) SB265610 or (C) CX4338 at the indicated concentrations for 10 min prior to CXCL8 (50 nM) treatment for additional 10 min. Cells were then stimulated with forskolin (50 μM) until maximum luminescence signal was reached (10–20 min). Data are normalized to baseline (before treatment with compounds) and a representative kinetic curve of three independent experiments is shown. (B) Maximum signal was used to calculate % inhibition of CXCL8-mediated forskolin cAMP production. Data are shown as mean ± SEM of at least three independent experiments. (D) Kinetic curve of longer compound treatment time. Cells were prepared as in (A)–(C). Cells were pre-treated with CX4338 for 1 h before CXCL8 (50 nM) and forskolin (50 μM) stimulation.

G-protein signalling (calcium mobilization and ERK1/2, p38 and JNK phosphorylation) was observed in CXCR2-β-arrestin1/2-deficient models (Richardson *et al.*, 2003; Su *et al.*, 2005). Zhao *et al.* (2004) also showed that enhanced CXCR2/G-protein signalling in β-arrestin1/2-deficient cells led to activation of stress kinases including JNK and p38 and subsequent NAPDH-oxidase (NOX)-dependent generation of ROS and cell death. Although we also observed p38 and JNK activation upon CX4338 treatment (Figure 6), we did not observe significant increase in ROS levels (Supporting Information Fig. S8), which might explain the lack of cell death observed during CX4338 treatment (Table 2). Perhaps, the effects of ROS-mediated cell death are dependent on NOX expression and thus cell line-dependent. The proposed mechanism of action of CX4338 is represented in a schematic diagram in Supporting Information Fig. S9.

It is also important to note that we used two different cell lines as models to assess the effects of CX4338 on β-arrestin-2 and G-protein signalling, which may contribute to the biased signalling observed. Due to the several limitations of the cell lines used, we could not perform all assays with the same cell lines. CXCR2-bla U2OS cells were used to assess β-arrestin-2 recruitment, receptor internalization and degradation, and chemotaxis, whereas 293T-CXCR2-GFP cells were used to assess the effects of CX4338 on CXCL8-mediated calcium mobilization, MAPK phosphorylation and cAMP signalling. However, the mRNA expression levels of CXCR2 in CXCR2-bla U2OS and 293T-CXCR2-GFP cells were comparable (115- and 224-fold increase compared with 293T parental cells, respectively; Supporting Information Fig. S10). It should be noted that mRNA transcript levels are not necessarily reflective of receptor expression. Additionally, the different effects on CXCR2 signalling of SB265610 and CX4338 on CXCL8-mediated G-protein signalling further suggest that the biased mechanism observed with CX4338 is unlikely to be due to different levels of overexpression of CXCR2 in the different models.

A counter-screen with CXCR4 Tango assay showed that CX4338 interacted with the CXCR2 receptor and not with β-arrestin-2. CXCR2 and CXCR4 belong to the same chemokine family and are activated by different ligands. Every component of the Tango assay was identical, except for chemokine expression and ligand activation. Thus, we would not anticipate selectivity in CXCR2/4 Tango assays if

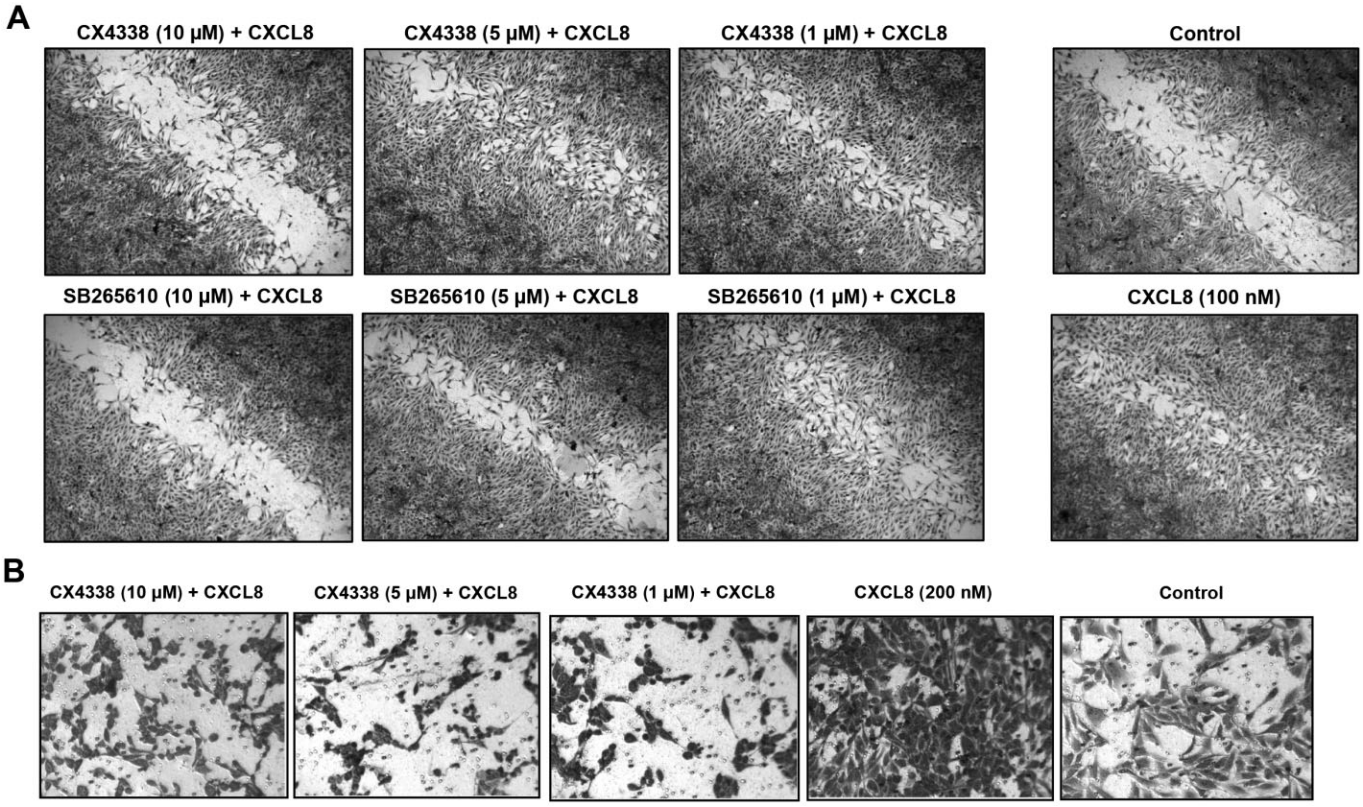

Figure 8

CX4338 inhibits CXCL8-mediated cell migration. (A) CXCR2-bla U2OS were seeded in 96-well plates at 30 000 cells per well in DMEM supplemented with 1% FBS overnight. A single wound was induced in the monolayer with a sterile pipette tip and washed with PBS. Cells were treated with CX4338 or SB265610 at 10, 5 and 1 μM and stimulated with CXCL8 (100 nM) for 24 h. Control wells were not stimulated with CXCL8. CXCL8 wells were treated with CXCL8 (100 nM). Representative images of two independent experiments performed in duplicate are shown here. (B) CXCR2-bla U2OS cells were seeded on 24-well transwell inserts at 100 000 cells per well in DMEM supplemented with 1% FBS overnight. The next day, cells were treated with 10, 5, 1 μM of CX4338 and stimulated with CXCL8 (200 nM) for 48 h.

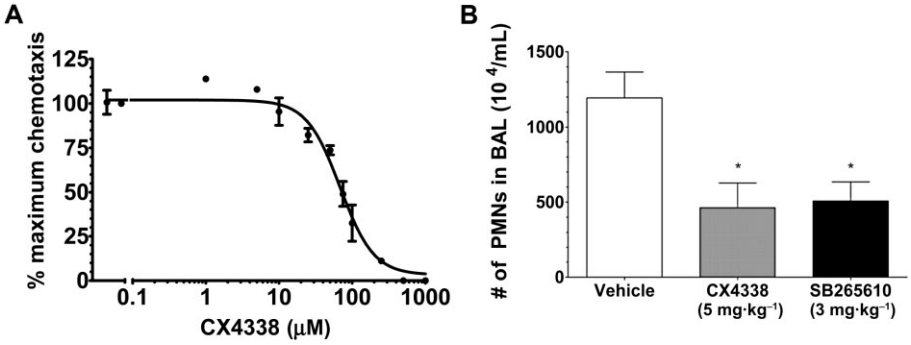

Figure 9

CX4338 inhibits PMN migration in LPS-induced inflammation model. (A) Concentration-dependent inhibition of human neutrophil chemotaxis. Neutrophils were incubated with CX4338 for 1 h, and placed in the upper wells of a chemotaxis plate containing 50 nM of CXCL8 in the lower wells. Neutrophils were allowed to migrate for 2–4 h at 37°C and 5% CO_2. Inhibition of chemotaxis was evaluated based on cell counts relative to control (untreated with CXCL8). CX4338 concentration-dependently inhibited CXCL8-induced chemotaxis with an IC_{50} of 68.6 μM (95% CI 56.32–83.53, r^2 = 0.90). Results are mean ± SD of two to three experiments. (B) Attenuation of neutrophil recruitment in BALF at 24 h by pre-treatment with CX4338 before intranasal LPS challenge of mice. CX4338 (5 mg·kg^{-1}, s.c.) significantly inhibited neutrophil influx. Results are mean ± SD of three animals per treatment group (n = 9). *P < 0.05.

β-arrestin-2 were the target of inhibition. CX4338 selectively inhibited CXCR2/β-arrestin-2 recruitment over CXCR4/β-arrestin-2 recruitment (selectivity was greater than 16; Table 1), providing evidence that CX4338 selectively interacts with CXCR2 and not with CXCR4. Thus, the effects of CX4338 observed in CXCR2/β-arrestin-2 and G-protein signalling is not likely to be due to non-specific β-arrestin-2 inhibition, but may involve the upstream phosphorylation of the CXCR2 receptor via GRK6. Further work will be required to confirm this.

These studies also show that selective inhibition of CXCR2-mediated β-arrestin-2 signalling by CX4338 was sufficient to inhibit CXCL8-mediated *in vitro* chemotaxis (Figures 8 and 9), which is consistent with previous experiments with β-arrestin1/2-deficient models (Richardson *et al.*, 2003; Raghuwanshi *et al.*, 2012). Importantly, CX4338 also significantly reduced LPS-stimulated chemotaxis of neutrophils into BAL in mice (Figure 9B), which is contrary to previous studies that showed β-arrestin1/2 deficiency up-regulated CXCL1-mediated chemotaxis in *in vivo* mice models (dorsal air pouch and excisional wound healing assay) (Su *et al.*, 2005; Raghuwanshi *et al.*, 2012). The observed discrepancy might be due to different *in vivo* models used to assess chemotaxis.

In conclusion, we have identified a distinct class of compounds that alters CXCL8/CXCR2 signalling with a unique mechanism of action that shows promising anti-inflammatory therapeutic potential. CX4338 altered CXCR2 signalling by inhibiting CXCR2/β-arrestin-2 coupling while up-regulating CXCR2-mediated MAPK activation. We also demonstrate inhibition of CXCR2/β-arrestin-2 coupling was sufficient to inhibit CXCL8-mediated chemotaxis *in vitro* and *in vivo*. CX4338 can also be used as a mechanistic marker to understand the role of CXCR2/β-arrestin-2 signalling and warrants further optimization and development.

Acknowledgements

This study was funded by the Department of Defense Lung Cancer Research Program, Grant No. LC090363 (N. N.) and the Webb Foundation (PMB). Research reported in this publication was also supported by the NIDCR under Training Award Number 5T90DE021982-02 (T. B.). The content is solely the responsibility of the authors and does not necessarily represent the official views of the National Institutes of Health. We thank Dr Daryl Davies for kindly generating the 293T-CXCR2-GFP cell lines and Dr Zack Howard for providing the HEK293-HA-CXCR2-GFP-β-arrestin-2 cell lines. We also thank Dr Shili Xu for his assistance and artistic drawing of the schematic presented in Supporting Information Fig. S9.

Conflict of interest

None.

References

Aaron SD, Angel JB, Lunau M, Wright K, Fex C, Le Saux N *et al.* (2001). Granulocyte inflammatory markers and airway infection during acute exacerbation of chronic obstructive pulmonary disease. Am J Respir Crit Care Med 163: 349–355.

Alexander SPH, Benson HE, Faccenda E, Pawson AJ, Sharman JL, Spedding M *et al.* (2013), The Concise Guide to PHARMACOLOGY 2013/14: G Protein-Coupled Receptors. Br J Pharmacol 170: 1459–1581.

Altenburg JD, Broxmeyer HE, Jin Q, Cooper S, Basu S, Alkhatib G (2007). A naturally occurring splice variant of CXCL12/stromal cell-derived factor 1 is a potent human immunodeficiency virus type 1 inhibitor with weak chemotaxis and cell survival activities. J Virol 81: 8140–8148.

Aul R, Patel S, Summerhill S, Kilty I, Plumb J, Singh D (2012). LPS challenge in healthy subjects: an investigation of neutrophil chemotaxis mechanisms involving CXCR1 and CXCR2. Int Immunopharmacol 13: 225–231.

Baggiolini M, Dewald B, Moser B (1997). Human chemokines: an update. Annu Rev Immunol 15: 675–705.

Balabanian K, Lagane B, Pablos JL, Laurent L, Planchenault T, Verola O *et al.* (2005). WHIM syndromes with different genetic anomalies are accounted for by impaired CXCR4 desensitization to CXCL12. Blood 105: 2449–2457.

Barlic J, Khandaker MH, Mahon E, Andrews J, Devries ME, Mitchell GB *et al.* (1999). beta-Arrestins regulate interleukin-8-induced CXCR1 internalization. J Biol Chem 274: 16287–16294.

Barnes PJ (2000). Chronic obstructive pulmonary disease. N Engl J Med 343: 269–280.

Barnes PJ (2004). Mediators of chronic obstructive pulmonary disease. Pharmacol Rev 56: 515–548.

Bertini R, Allegretti M, Bizzarri C, Moriconi A, Locati M, Zampella G *et al.* (2004). Noncompetitive allosteric inhibitors of the inflammatory chemokine receptors CXCR1 and CXCR2: prevention of reperfusion injury. Proc Natl Acad Sci U S A 101: 11791–11796.

Bradley ME, Bond ME, Manini J, Brown Z, Charlton SJ (2009). SB265610 is an allosteric, inverse agonist at the human CXCR2 receptor. Br J Pharmacol 158: 328–338.

Busch-Petersen J (2006). Small molecule antagonists of the CXCR2 and CXCR1 chemokine receptors as therapeutic agents for the treatment of inflammatory diseases. Curr Top Med Chem 6: 1345–1352.

Catusse J, Liotard A, Loillier B, Pruneau D, Paquet JL (2003). Characterization of the molecular interactions of interleukin-8 (CXCL8), growth related oncogen alpha (CXCL1) and a non-peptide antagonist (SB 225002) with the human CXCR2. Biochem Pharmacol 65: 813–821.

Chapman RW, Minnicozzi M, Celly CS, Phillips JE, Kung TT, Hipkin RW *et al.* (2007). A novel, orally active CXCR1/2 receptor antagonist, Sch527123, inhibits neutrophil recruitment, mucus production, and goblet cell hyperplasia in animal models of pulmonary inflammation. J Pharmacol Exp Ther 322: 486–493.

Chapman RW, Phillips JE, Hipkin RW, Curran AK, Lundell D, Fine JS (2009). CXCR2 antagonists for the treatment of pulmonary disease. Pharmacol Ther 121: 55–68.

Fan GH, Yang W, Wang XJ, Qian Q, Richmond A (2001). Identification of a motif in the carboxyl terminus of CXCR2 that is involved in adaptin 2 binding and receptor internalization. Biochemistry 40: 791–800.

Fan GH, Lapierre LA, Goldenring JR, Richmond A (2003). Differential regulation of CXCR2 trafficking by Rab GTPases. Blood 101: 2115–2124.

Hall DA, Beresford IJ, Browning C, Giles H (1999). Signalling by CXC-chemokine receptors 1 and 2 expressed in CHO cells: a comparison of calcium mobilization, inhibition of adenylyl cyclase and stimulation of GTPgammaS binding induced by IL-8 and GROalpha. Br J Pharmacol 126: 810–818.

Holz O, Khalilieh S, Ludwig-Sengpiel A, Watz H, Stryszak P, Soni P *et al.* (2010). SCH527123, a novel CXCR2 antagonist, inhibits ozone-induced neutrophilia in healthy subjects. Eur Respir J 35: 564–570.

Hristov M, Zernecke A, Liehn EA, Weber C (2007). Regulation of endothelial progenitor cell homing after arterial injury. Thromb Haemost 98: 274–277.

Hunt F, Austin C, Austin R, Bonnert R, Cage P, Christie J *et al.* (2007). SAR studies on thiazolo[4,5-d]pyrimidine based CXCR2 antagonists involving a novel tandem displacement reaction. Bioorg Med Chem Lett 17: 2731–2734.

Jacobs JP, Ortiz-Lopez A, Campbell JJ, Gerard CJ, Mathis D, Benoist C (2010). Deficiency of CXCR2, but not other chemokine receptors, attenuates autoantibody-mediated arthritis in a murine model. Arthritis Rheum 62: 1921–1932.

Keatings VM, Collins PD, Scott DM, Barnes PJ (1996). Differences in interleukin-8 and tumor necrosis factor-alpha in induced sputum from patients with chronic obstructive pulmonary disease or asthma. Am J Respir Crit Care Med 153: 530–534.

Kilkenny C, Browne WJ, Cuthill IC, Emerson M, Altman DG (2010). Improving bioscience research reporting: the ARRIVE guidelines for reporting animal research. Plos Biol 8: e1000412.

de Kruijf P, Van Heteren J, Lim HD, Conti PG, Van Der Lee MM, Bosch L *et al.* (2009). Nonpeptidergic allosteric antagonists differentially bind to the CXCR2 chemokine receptor. J Pharmacol Exp Ther 329: 783–790.

de Kruijf P, Lim HD, Roumen L, Renjaan VA, Zhao J, Webb ML *et al.* (2011). Identification of a novel allosteric binding site in the CXCR2 chemokine receptor. Mol Pharmacol 80: 1108–1118.

Lazaar AL, Sweeney LE, Macdonald AJ, Alexis NE, Chen C, Tal-Singer R (2011). SB-656933, a novel CXCR2 selective antagonist, inhibits ex vivo neutrophil activation and ozone-induced airway inflammation in humans. Br J Clin Pharmacol 72: 282–293.

McGrath JC, Drummond GB, McLachlan EM, Kilkenny C, Wainwright CL (2010). Guidelines for reporting experiments involving animals: the ARRIVE guidelines. Br J Pharmacol 160: 1573–1576.

Nair P, Gaga M, Zervas E, Alagha K, Hargreave FE, O'Byrne PM *et al.* (2012). Safety and efficacy of a CXCR2 antagonist in patients with severe asthma and sputum neutrophils: a randomized, placebo-controlled clinical trial. Clin Exp Allergy 42: 1097–1103.

Nasser MW, Raghuwanshi SK, Malloy KM, Gangavarapu P, Shim JY, Rajarathnam K *et al.* (2007). CXCR1 and CXCR2 activation and regulation. Role of aspartate 199 of the second extracellular loop of CXCR2 in CXCL8-mediated rapid receptor internalization. J Biol Chem 282: 6906–6915.

Nasser MW, Raghuwanshi SK, Grant DJ, Jala VR, Rajarathnam K, Richardson RM (2009). Differential activation and regulation of CXCR1 and CXCR2 by CXCL8 monomer and dimer. J Immunol 183: 3425–3432.

Raghuwanshi SK, Su Y, Singh V, Haynes K, Richmond A, Richardson RM (2012). The chemokine receptors CXCR1 and CXCR2 couple to distinct G protein-coupled receptor kinases to mediate and regulate leukocyte functions. J Immunol 189: 2824–2832.

Rajagopal S, Kim J, Ahn S, Craig S, Lam CM, Gerard NP *et al.* (2010a). Beta-arrestin- but not G protein-mediated signaling by the 'decoy' receptor CXCR7. Proc Natl Acad Sci U S A 107: 628–632.

Rajagopal S, Rajagopal K, Lefkowitz RJ (2010b). Teaching old receptors new tricks: biasing seven-transmembrane receptors. Nat Rev Drug Discov 9: 373–386.

Reiter E, Ahn S, Shukla AK, Lefkowitz RJ (2012). Molecular mechanism of β-arrestin-biased agonism at seven-transmembrane receptors. Annu Rev Pharmacol Toxicol 52: 179–197.

Richardson RM, Marjoram RJ, Barak LS, Snyderman R (2003). Role of the cytoplasmic tails of CXCR1 and CXCR2 in mediating leukocyte migration, activation, and regulation. J Immunol 170: 2904–2911.

Salchow K, Bond ME, Evans SC, Press NJ, Charlton SJ, Hunt PA *et al.* (2010). A common intracellular allosteric binding site for antagonists of the CXCR2 receptor. Br J Pharmacol 159: 1429–1439.

Schild HO (1947). pA, a new scale for the measurement of drug antagonism. Br J Pharmacol Chemother 2: 189–206.

Stillie R, Farooq SM, Gordon JR, Stadnyk AW (2009). The functional significance behind expressing two IL-8 receptor types on PMN. J Leukoc Biol 86: 529–543.

Su Y, Raghuwanshi SK, Yu Y, Nanney LB, Richardson RM, Richmond A (2005). Altered CXCR2 signaling in beta-arrestin-2-deficient mouse models. J Immunol 175: 5396–5402.

Suratt BT, Petty JM, Young SK, Malcolm KC, Lieber JG, Nick JA *et al.* (2004). Role of the CXCR4/SDF-1 chemokine axis in circulating neutrophil homeostasis. Blood 104: 565–571.

Tanino M, Betsuyaku T, Takeyabu K, Tanino Y, Yamaguchi E, Miyamoto K *et al.* (2002). Increased levels of interleukin-8 in BAL fluid from smokers susceptible to pulmonary emphysema. Thorax 57: 405–411.

Traves SL, Smith SJ, Barnes PJ, Donnelly LE (2004). Specific CXC but not CC chemokines cause elevated monocyte migration in COPD: a role for CXCR2. J Leukoc Biol 76: 441–450.

White JR, Lee JM, Young PR, Hertzberg RP, Jurewicz AJ, Chaikin MA *et al.* (1998). Identification of a potent, selective non-peptide CXCR2 antagonist that inhibits interleukin-8-induced neutrophil migration. J Biol Chem 273: 10095–10098.

Woolhouse IS, Bayley DL, Stockley RA (2002). Sputum chemotactic activity in chronic obstructive pulmonary disease: effect of alpha(1)-antitrypsin deficiency and the role of leukotriene B(4) and interleukin 8. Thorax 57: 709–714.

Yamamoto C, Yoneda T, Yoshikawa M, Fu A, Tokuyama T, Tsukaguchi K *et al.* (1997). Airway inflammation in COPD assessed by sputum levels of interleukin-8. Chest 112: 505–510.

Yang W, Wang D, Richmond A (1999). Role of clathrin-mediated endocytosis in CXCR2 sequestration, resensitization, and signal transduction. J Biol Chem 274: 11328–11333.

Zhao M, Wimmer A, Trieu K, Discipio RG, Schraufstatter IU (2004). Arrestin regulates MAPK activation and prevents NADPH oxidase-dependent death of cells expressing CXCR2. J Biol Chem 279: 49259–49267.

Supporting information

Additional Supporting Information may be found in the online version of this article at the publisher's web-site:

http://dx.doi.org/10.1111/bph.12547

Figure S1 Chemical structures of CX compounds identified from screening. Compounds were purchased from Enamine.
Figure S2 CX4338 does not show toxicity in NSCLC and Tango™ CXCR2/4 cell lines. (A) H460, H1299, CXCR2/4-U2OS cells treated with compounds at 100, 10 and 1 μM for 72 h and cell viability was measured using MTT assay. (B) Colony formation of H1299 cells treated with CX4338 at indicated doses. (C) Colony formation of HCT116p53+/+ and –/– cells treated with CX4338 at indicated doses.
Figure S3 CXCL8 induces CXCR2 internalization in a time and dose-dependent manner. (A) Surface expression of CXCR2 in CXCR2-bla U2OS cells treated with various concentrations of CXCL8 (0–100 nM) for various time points (0–300 min). IgG wells were not stimulated with CXCL8 and was incubated with mouse IgG instead of CXCR2 antibodies as a negative control. CXCR2 expression is detected using the IR680 channel on the Licor Odyssey. (B) CXCL8 dose-dependently induced receptor internalization. Quantitation of A and plotted as log (CXCL8 concentrations) versus percent receptor internalized. (C) CXCL8 induced receptor internalization in a time-dependent manner. Quantitation of A and plotted as time vs. percent receptor internalized.
Figure S4 CXCL8 induces CXCR2 turnover in CXCR2-bla U2OS cells. (A) Total expression of CXCR2 treated with various concentrations of CXCL8 (1–100 nM) for various time points (0–300 min). Lanes 1–8 were permeabilized to detect total CXCR2 expression. Lane 9 was not permeabilized to detect surface CXCR2 expression in unstimulated cells. (B) CXCL8 dose-dependently induces receptor degradation. Quantitation of A and represented as log of CXCL8 concentrations versus percent receptor degraded. (C) CXCL8 induced receptor degradation in a time-dependent manner. Quantitation of A and represented as time versus percent receptor internalized.
Figure S5 CXCL8 inhibits forskolin-stimulated cAMP signalling. 293T-CXCR2-GFP-p22F cells were pre-treated with CXCL8 at 50 nM for 10 min and stimulated with forskolin (50 μM) for 15–20 min until the maximum signal was reached. cAMP production was detected using the GloSensor luciferase assay (luminescence based). Data represent mean ± SD of maximum cAMP produced upon treatment with forskolin and/or CXCL8.
Figure S6 CX4338 inhibits neutrophil migration. Concentration-dependent inhibition of human neutrophil chemotaxis. Neutrophils were incubated with CX4338 for 1 h, and then placed in the top wells of a chemotaxis plate containing 50 nM of CXCL8 in the bottom wells. Neutrophils were allowed to chemotax for 2–4 h at 37°C and 5% CO_2. Inhibition of chemotaxis was evaluated based on cell counts relative to control (untreated with CXCL8). CX4338 significantly inhibited neutrophil chemotaxis at 50 and 100 μM (*$P < 0.05$). Results are shown as total migrated neutrophils when incubated with CX4338 in a representative experiment.
Figure S7 CX4338 inhibits CXCR2 in a non-competitive manner in the CXCR2 Tango assay. CXCR2-bla U2OS cells were co-treated with a fixed dose of CX4338 (20, 10, 8, 6, 2 or 1 μM) and various concentrations of CXCL8 ranging from 1000 to 0.1 nM. (A) The inhibitory effects of CX4338 were reduced with increasing concentrations of ligand, suggesting that response is ligand-dependent. Though it does not appear that maximum CXCL8 stimulation was achieved when cells were pre-treated with CX4338 at 20, 10 and 8 μM, curve-fitting analysis of CXCL8 dose–response curves in the presence of lower CX4338 concentrations demonstrate that CX4338 reduced maximum ligand-induced response, suggesting that CX4338 may act as a non-competitive inhibitor. (B) Schild plot analysis suggests CX4338 inhibits CXCR2 in a non-competitive manner. Treatment curves with 20, 10 and 8 μM of CX4338 were excluded from this analysis as we could not determine the maximum response and could not accurately calculate the EC_{50}. Plotting –log B versus log[(A′/A)], we calculated a Schild slope of 1.479 with an R^2 of 0.99. Our data did not produce a slope of 1, which further indicates CX4338 does not inhibit CXCR2 in competitive manner.
Figure S8 Effects of CX4338 on ROS levels. 293T-CXCR2-GFP cells were seeded in 96-well plates at 100 000 cells per well overnight. Cells were treated with CX4338, SB265610 or 0.5% DMSO (vehicle control) with or without 25 μM of DCF dye for 30 min in PBS at 37°C. Cells were removed from plate and read on flow cytometer to detect oxidized DCF.
Figure S9 Proposed mechanism of CX4338. CX4338 selectively inhibits CXCL8-induced β-arrestin-2 recruitment and subsequent receptor internalization, recycling and degradation. Receptor recycling and degradation negatively regulates CXCR2-mediated G-protein signalling. However, selective inhibition of CXCR2/β-arrestin-2 signalling via CX4338 leads to sustained and enhanced CXCR2-mediated G-protein signalling which include MAP kinases (JNK1 and ERK), calcium mobilization from the ER to the cytoplasm, and adenylyl cyclase inhibition.
Figure S10 mRNA expression of CXCR2 in cell line models and human neutrophils. Fold increase in CXCR2 mRNA expression were normalized to 293T parental cell lines. 293T-CXCR2-GFP cell lines showed a 115-fold increase in CXCR2 expression compared to 293T cells. CXCR2-bla U2OS cells showed a 224-fold increase in CXCR2 expression compared to 293T cells. Human neutrophils extracted from healthy volunteers showed a 3364-fold increase in CXCR2 expression compared to 293T cells. Data represent mean ± SD of two experiments.
Table S1 IC_{50} values for CXCR2/4 Tango™ inhibition for CX compounds identified in HTS screen.
Table S2 Schild plot analysis of CX4338.